MPMI Vol. 35, No. 9, 2022, pp. 779–790, https://doi.org/10.1094/MPMI-12-21-0301-R

A *Phakopsora pachyrhizi* Effector Suppresses PAMP-Triggered Immunity and Interacts with a Soybean Glucan Endo-1,3-β-Glucosidase to Promote Virulence

Thays V. Bueno,[1] Patrícia P. Fontes,[2] Valeria Y. Abe,[3] Alice Satiko Utiyama,[1] Renato L. Senra,[2] Liliane S. Oliveira,[3,4] Adriana Brombini dos Santos,[3] Everton G. Capote Ferreira,[3] Luana M. Darben,[5] Aluízio Borém de Oliveira,[1] Ricardo V. Abdelnoor,[3] Steven A. Whitham,[6] Luciano G. Fietto,[2] and Francismar C. Marcelino-Guimarães[3,†]

[1] Department of Agronomy, Federal University of Viçosa, Viçosa, Minas Gerais, CEP 36570-900, Brazil
[2] Department of Biochemistry and Molecular Biology, Federal University of Viçosa, Viçosa, Minas Gerais, CEP 36570-900, Brazil
[3] Embrapa soja, Plant Biotechnology, Londrina, Paraná, CEP 70770-901, Brazil
[4] Department of Computer Science, Federal University of Technology - Paraná (UTFPR), Cornélio Procópio, Paraná 86300-000, Brazil
[5] Corteva Agriscience, Palmas, Tocantins, CEP, Brazil
[6] Department of Plant Pathology and Microbiology, Iowa State University, Ames, IA 50011, U.S.A.

Accepted for publication 23 April 2022.

Asian soybean rust, caused by the fungus *Phakopsora pachyrhizi*, is one of the most important diseases affecting soybean production in tropical areas. During infection, *P. pachyrhizi* secretes proteins from haustoria that are transferred into plant cells to promote virulence. To date, only one candidate *P. pachyrhizi* effector protein has been characterized in detail to understand the mechanism by which it suppresses plant defenses to enhance infection. Here, we aimed to extend understanding of the pathogenic mechanisms of *P. pachyrhizi* based on the discovery of host proteins that interact with the effector candidate Phapa-7431740. We demonstrated that Phapa-7431740 suppresses pathogen-associated molecular pattern-triggered immunity (PTI) and that it interacts with a soybean glucan endo-1,3-β-glucosidase (GmβGLU), a pathogenesis-related (PR) protein belonging to the PR-2 family. Structural and phylogenetic characterization of the PR-2 protein family predicted in the soybean genome and comparison to PR-2 family members in *Arabidopsis thaliana* and cotton, demonstrated that GmβGLU is a type IV β-1,3-glucanase. Transcriptional profiling during an infection time course showed that the *GmβGLU* mRNA is highly induced during the initial hours after infection, coinciding with peak of expression of Phapa-7431740. The effector was able to interfere with the activity of GmβGLU in vitro, with a dose-dependent inhibition. Our results suggest that Phapa-7431740 may suppress PTI by interfering with glucan endo-1,3-β-glucosidase activity.

Keywords: *Glycine max*, protein-protein interaction, rust effectors

Asian soybean rust (ASR) caused by the biotrophic fungus *Phakopsora pachyrhizi* (Sydow & Sydow) is one of the most important diseases affecting soybean production. Since the first report of its occurrence in Brazil in 2001, Asian soybean rust has caused significant damage to soybeans leading to severe economic impacts (Godoy et al. 2016). There are seven genetic loci conferring resistance to *P. pachyrhizi* named *Rpp1* to *Rpp7*, which can effectively protect soybean plants against avirulent isolates (Bromfield and Hartwig 1980; Childs et al. 2018; Garcia et al. 2008; Hartwig 1986; Hidayat and Somaatmadja 1977; Li et al. 2012; Singh and Thapliyal 1977). However, *P. pachyrhizi*, like other rust fungi, can rapidly adapt to overcome the resistance provided by single genes (Aime et al. 2017). Therefore, understanding the biological and molecular mechanisms that *P. pachyrhizi* utilizes to infect soybean is expected to be important for developing novel strategies for controlling ASR (Rincão et al. 2018).

At the present time, the majority of knowledge on the molecular interactions of soybean and *P. pachyrhizi* have focused mainly on transcriptome analyses that have identified differentially expressed genes in soybean during infection in compatible and incompatible interactions (Elmore et al. 2020; Hossain et al. 2018; Morales et al. 2013; Panthee et al. 2007; Schneider et al. 2011; van de Mortel et al. 2007). Some studies have used proteomics analysis to identify proteins of the fungus present during the germination of urediniospores (Luster et al. 2010) and specific proteins in the appressorial stage (Stone et al. 2012).

[†]Corresponding author: F. C. Marcelino-Guimarães; francismar.marcelino@embrapa.br

Funding: This study was financed by the Brazilian Agricultural Research Corporation (EMBRAPA) and by the Coordenação de Aperfeiçoamento de Pessoal de Nível Superior–Brasil (CAPES), Finance Code 001 for a scholarship.

e-Xtra: Supplementary material is available online.

The author(s) declare no conflict of interest.

The author(s) have dedicated the work to the public domain under the Creative Commons CC0 "No Rights Reserved" license by waiving all of his or her rights to the work worldwide under copyright law, including all related and neighboring rights, to the extent allowed by law, 2022.

The *P. pachyrhizi* secretome was first described from the analysis of RNA-Seq using samples extracted from the haustoria (Link et al. 2014). Later, this secretome was expanded to 851 candidate proteins when it combined laser capture microdissection of lesions and RNA-Seq (Carvalho et al. 2017). Recently, a de novo transcriptome of *P. pachyrhizi* was assembled that combined short-read (Illumina RNA-Seq) with long-read (PacBio Iso-Seq) sequencing data, which was also used to identify putative effectors during infection (Elmore et al. 2020). Only a few of the candidate effectors predicted from these transcriptome studies have been shown to have effector-like activities. Two candidates for *P. pachyrhizi* effectors (CSEP-07 and CSEP-09) were able to increase the infection of *Phytophthora infestans* in tobacco leaves, suggesting a role in the virulence of the soybean rust fungus (Kunjeti et al. 2016). To validate *P. pachyrhizi* effector candidates (PpECs) on a large scale, a study utilizing different heterologous expression systems demonstrated that 17 PpECs out of 82 tested were able to suppress basal defense responses associated with pathogen-associated molecular pattern-triggered immunity (PTI) (Qi et al. 2018). Currently, only one effector candidate, PpEC23, and its host interactor have been identified and characterized at the molecular level. PpEC23 interacted with the soybean transcription factor (*GmSPL12l*) in yeast and in plant cells, and it was suggested that PpEC23 may interfere directly with the function or post-translational regulation of *GmSPL12l* (Qi et al. 2016).

The *P. pachyrhizi* effector candidate (de_novo_3939) suppressed effector-triggered immunity (ETI) responses to *Pseudomonas syringae* pv. *tomato* DC3000 in tobacco leaves. Hierarchical cluster analysis of families of candidate secreted proteins encoded by rust fungi placed de_novo_3939 in a family (family 3), which contains members that are secreted, small, cysteine-rich proteins that also possess potentially conserved motifs, [AFY] xC and [FY] xC (Carvalho et al. 2017). These motifs have been described as important in translocation of effector proteins across the fungal extrahaustorial membrane among candidates encoded by rust fungi (Godfrey et al. 2010; Saunders et al. 2012).

Based on the reference genome of the isolate MT2006 of *P. pachyrhizi* recently released by the Joint Genome Institute (JGI), de_novo_3939 was identified as corresponding to the gene model Phapa-7431740, confirming the coding sequence predicted in our previous study (Carvalho et al. 2017). This gene encodes a protein of 121 amino acids that contains the calcium-binding epidermal growth factor (EGF) domain (PF07645.16). Here, we demonstrated that Phapa-7431740 targets a soybean glucan endo-1,3-β-glucosidase (GmβGLU) and it interferes with the activity of this enzyme. GmβGLU is a pathogenesis-related (PR) protein, and its expression is induced by pathogens, including *P. pachyrhizi*, in soybean. Our results support the hypothesis that Phapa-7431740 is an effector that disrupts the function of an antifungal PR protein (GmβGLU) to promote *P. pachyrhizi* infection of soybean.

RESULTS

In silico characterization of the effector candidate Phapa-7431740.

The de_novo_3939 transcript was aligned against the reference genome of *P. pachyrhizi* available at JGI (MT2006 genome), using the BLASTx program. To identify the gene model most similar to de_novo_3939, only proteins with more than 50% of coverage and above 70% identity were selected. The protein predicted by the Phapa-7431740 gene model was identical to the protein encoded by the transcript de_novo_3939 with 100% coverage and 100% amino acid identity. The Phapa-7431740 gene model has a nucleotide sequence of 1,415 bp with five exons and four introns. The coding sequence is 366 bp long and encodes a protein of 121 amino acids with an approximate mass of 12.66 kDa and containing 11 cysteine residues (9%). A signal peptide (SP) of 25 amino acid residues is predicted at the amino terminus by SignalP 5.0, and it also possesses the FxC motif and a calcium-binding EGF domain.

Phapa-7431740 suppresses pathogen-associated molecular pattern (PAMP)-related responses.

The production of reactive oxygen species (ROS) and callose deposition are important markers of basal defense responses to pathogen infection. To test if Phapa-7431740 suppresses basal defense responses, we expressed it from pEDV6 in *Pseudomonas fluorescens* Pf0-1 (EtHAn). EtHAn is a strain of non-pathogenic *Pseudomonas fluorescens* that was engineered to carry the type III secretion system and is able to secrete proteins fused to N-terminal type III secretion signals into plant cells (Chang et al. 2005). ROS and callose deposition were strongly elicited when *Nicotiana benthamiana* leaves were inoculated with EtHAn carrying the pEDV6 empty vector (Fig. 1A and C). In contrast, ROS accumulation and callose deposition was similar in leaves inoculated with EtHAn expressing Phapa-7431740 and mock-inoculated negative control plants (Fig. 1A and C). This result indicates that Phapa-7431740 has the ability to suppress the PAMP-related responses elicited by EtHAn. It was verified by t test that there was a difference ($P < 0.01$) between the treatments, indicating the ability of this effector to suppress the PAMP related responses (Fig. 1B and D).

Identification and characterization of interaction partners of the effector candidate Phapa-7431740.

Because Phapa-7431740 was able to suppress basal defense induced by EtHAn, we hypothesized that it may interact with one or more soybean proteins. To identify interacting proteins by yeast two-hybrid, Phapa-7431740 was cloned into the pDEST32 vector to create pBD-7431740. AH109 yeast cells transformed with BD-7431740 did not grow on the selective medium, demonstrating that it did not autoactivate expression of the reporter genes. BD-7431740 was screened against a soybean cDNA library expressed from the prey vector (Alves et al. 2011). A total of 76 clones grew on synthetic dropout (SD) medium in the absence of leucine, tryptophan, and histidine (SD −LEU−TRP−HIS). Of these 76 clones, ten grew on solid SD −LEU−TRP−HIS medium in the presence of 3-amino-1,2,4-triazole (3-AT). These clones were transferred to SD −LEU−TRP−HIS liquid medium for extraction of yeast plasmid DNA. PCR amplification was performed using the pEXP-AD-502 primers (Supplementary Table S1) to estimate the size of the prey cDNA inserts. One clone had more than one amplicon, which may indicate that more than one plasmid was present in the corresponding yeast clone. The sequences of the soybean cDNA plasmid inserts were used in BLASTn and BLASTx searches against the GenBank nonredundant database (Benson et al. 2014). The insert of clone AD-bbt3 was 97.3% similar to Glyma.15G142400 (GmβGLU), and its coding sequence was in-frame with the Gal4p DNA activation domain (AD).

To confirm the interaction, plasmid AD-bbt3 was transformed into AH109 yeast cells containing the BD-7431740 vector. The assays for activation of the *HIS3* and *LacZ* reporter genes were performed with the following clones: BD-7431740 + AD-bbt3, BD-7431740 + AD-empty, BD-empty + AD-empty, BD-E2 + AD-E2 (positive control). In the *HIS3* reporter assay, clones were plated in SD −LEU−TRP−HIS medium and varying the concentrations of 3-AT (Fig. 2A). Only the BD-E2 + AD-E2 (positive control) and BD-7431740 + AD-bbt3 clones grew in media supplemented with 3-AT. In the *LacZ* assay, these same

clones developed blue colonies (Fig. 2B). These assays indicated that there is an interaction between the Phapa-7431740 and GmβGLU proteins in yeast.

The gene encoding GmβGLU is 1,383 bp in length and has two exons and one intron, and the 1,113-bp coding sequence encodes a 370–amino acid protein with a mass of approximately 37 kDa. The protein has an N-terminal SP of 32 amino acids, and it is annotated as a glucan endo-1,3-β-D-glucosidase in the conserved glycoside hydrolase domain of family 17 (GH17) (JGI Phytozome database). The insert of the AD-bbt3 clone identified in the screening corresponds to the 876- to 1,317-bp region of the 1,383-bp messenger RNA (mRNA). This sequence overlaps with nucleotides 775 to 1,036 of the coding sequence, which corresponds to the C-terminus of the GH17 domain (Fig. 2C).

Following the yeast two-hybrid assays, we were able to confirm the interaction between Phapa-7431740 and GmβGLU, first by in-vitro pull-down assay and, then, by the influence of Phapa-7431740 on GmβGLU activity. For the in vitro pull-down assay, the recombinant proteins Phapa-7431740 and GmβGLU were produced in *Escherichia coli* BL21 (DE3)-pRare and ArcticExpress (D3), respectively. Soluble extracts were purified by affinity chromatography on a nickel column. Protein purity was analyzed by sodium dodecyl sulfate-polyacrylamide gel electrophoresis (SDS-PAGE) and Western blotting (Fig. 3A and B). After purification, Phapa-7431740 was bound to Pierce NHS-activated magnetic beads, and, after blocking the unbound sites, the Phapa-7431740-bead complex was incubated with GmβGLU for 6 and 16 h. The interaction was permitted in the presence of 1 mM $CaCl_2$, and it was confirmed by the presence of two bands in the same lane (Fig. 3C). We observed a band of approximately 37 kDa that corresponds to GmβGLU in the second lane, indicating a specific interaction with Phapa-7431740 (the band of 15 kDa).

To better understand the functional role of this interaction, the activity of GmβGLU in the presence of the protein Phapa-7431740 was measured. The presence of the effector was able to interfere with the activity of GmβGLU (Fig. 3D). The activity was lower in the presence of Phapa-7431740 ($P < 0.01$), with a dose-dependent inhibition. In addition to these treatments, the assay was performed in the same way using an unrelated protein (bovine serum albumin [BSA]) as a control, which did not inhibit GmβGLU activity (Supplementary Fig. S1).

Characterization of the PR-2 soybean family.

To identify soybean PR-2 family members, we searched the soybean genome (Wm82.a4) using the PFAM model PF00332 (GH17) with a hidden Markov model (HMM) search program (Eddy 2011). Based on this strategy, 91 genes encoding the GH17 domain were identified. Subsequently, the 91 soybean protein sequences along with 67 cotton protein sequences and 50 protein sequences of *A. thaliana* were used to construct a phylogenetic tree.

The phylogenetic analysis classified the PR-2 family members into eight subfamilies (A through H) (Fig. 4A) with a maximum of 45 members in subfamily F, followed by subfamilies E and D, with 38 and 37 members, respectively (Supplementary

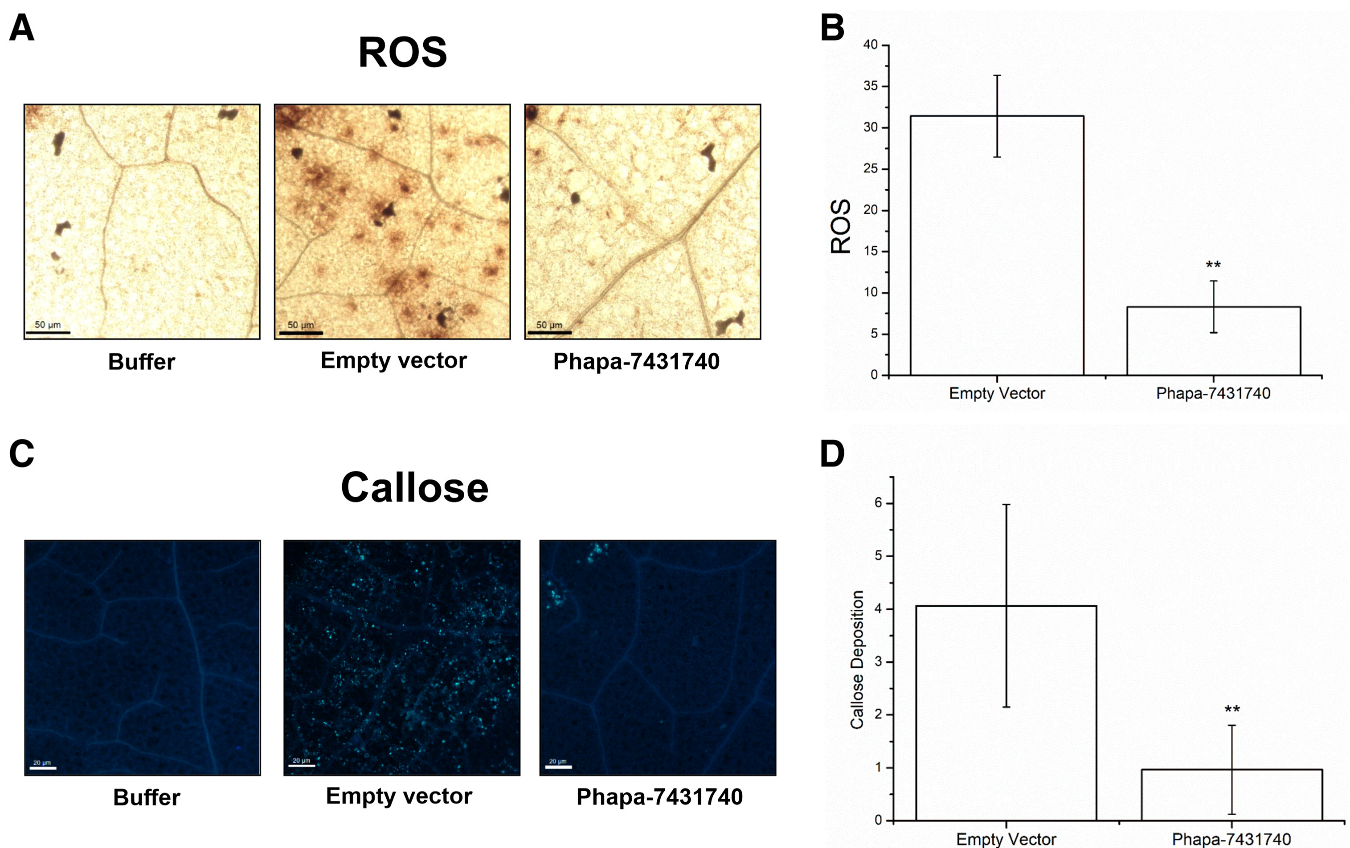

Fig. 1. Suppression of defense responses associated with pathogen-associated molecular pattern-triggered immunity. *Nicotiana benthamiana* leaves infiltrated with negative control ($MgCl_2$), positive control (*Pseudomonas fluorescens* EtHAn with empty pEDV6) and *Pseudomonas fluorescens* expressing Phapa-7431740 from pEDV6. **A,** Reactive oxygen species (ROS) were identified by staining with 3,3′-diaminobenzidine (DAB). Bars = 50 µm. **B,** Quantification of DAB staining for *Pseudomonas fluorescens* carrying the pEDV6 empty vector and *Pseudomonas fluorescens* expressing Phapa-7431740. **C,** Callose deposition was identified using aniline blue staining. Bars = 20 µm. **D,** Aniline blue staining graph for callose deposition for *Pseudomonas fluorescens* carrying the pEDV6 empty vector and *Pseudomonas fluorescens* expressing Phapa-7431740. Two asterisks (**) indicate significant differences at $P < 0.01$, as determined by the *t* test. The experiment was conducted with nine replicates, with one plant per replicate in a completely randomized experimental design.

Table S2). Subfamily H was composed of only five members, one from soybean and two each from cotton and *Arabidopsis*. In addition, the genes Glyma.15G242125 (which contains partial F-box and GH17 domains) and Gorai.008G159300 were classified as outgroups.

Studies of PR-2 family proteins from different species have been based on the classification proposed for PR-2 in tobacco (Doxey et al. 2007; Xu et al. 2016), which were placed into five classes (I to V) according to the protein domain architectures (Linthorst et al. 1990) (Fig. 4B). These classes are differentiated by the presence or absence of the X8 domain and the hydrophobic C-terminal sequence (CTS). The X8 domain was defined as a new class of carbohydrate-binding module of family 43 (CBM43) (Barral et al. 2005). The CTS corresponds to one or both a vacuolar targeting signal (Sticher et al. 1992) and the presence of a glycosidylphosphatidyllinositol (GPI) anchor (Borner et al. 2002). In addition to the five tobacco classes, we observed five other types of protein domain architectures in soybean proteins (Fig. 4C). The five additional types that have been observed in soybean are presented as variations of the tobacco classification.

Only subfamilies A and E have all members that lack the X8 domain (PF07983). Of the 91 soybean members, 44 do not have the CTS and 21 do not have the SP (Supplementary Table S3). The GmβGLU protein interacting with Phapa-7431740 was classified in subfamily E along with 15 other soybean, 11 cotton, and 11 *Arabidopsis* sequences (Fig. 4A). As for the classification based on the protein domain architectures, GmβGLU belongs to class IV.

Regarding the proteins with variation belonging to the different classes, the variation in classes I, II, and V are only the absence of the SP. The absence of SP can be due to protein annotation errors if the methionine start codon is not present. Whereas in class III, two variations were observed, namely, one protein showing the addition of the CTS and another protein showing both the addition of CTS and absence of N-terminal signal sequence (NTS). Furthermore, in class III, no soybean protein was identified with the protein domain architecture described for this class, only in each variation within class III was found one soybean protein (Supplementary Table S3).

Expression profile of GmβGLU in susceptible and resistant soybean genotypes infected with *P. pachyrhizi*.

The expression of the GmβGLU was analyzed by reverse transcription-quantitative PCR (RT-qPCR) in the susceptible (BRS 184) and resistant (*Rpp5*) soybean accessions infected by *P. pachyrhizi*. To confirm the occurrence of the infection, the presence of symptoms was verified 14 days after inoculation

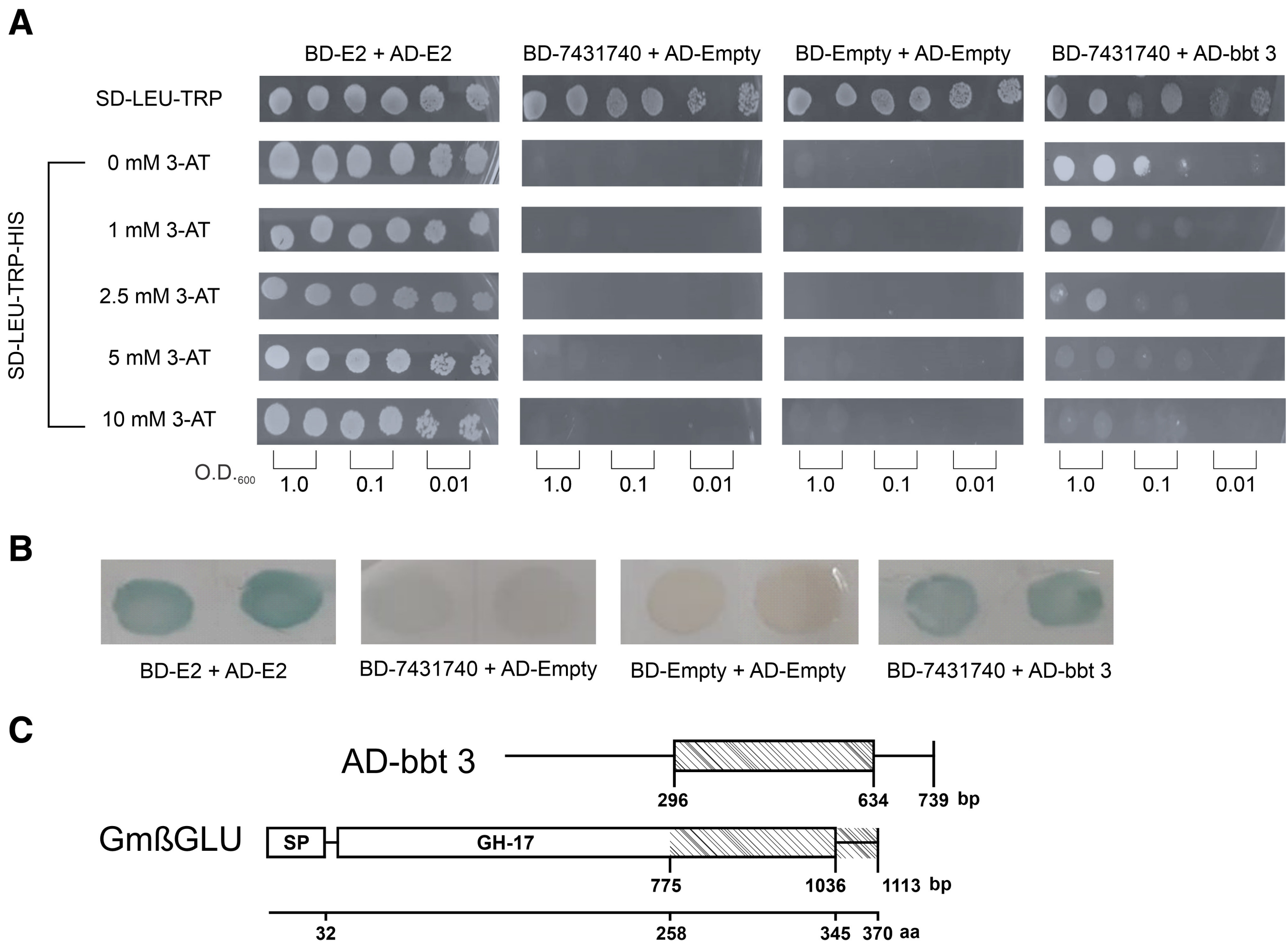

Fig. 2. Phapa-7431740 interacts with GmβGLU in the yeast two-hybrid assay. **A,** HIS3 reporter gene assay with clones BD-7431740 + AD-bbt3, BD-7431740 + AD-empty (negative control), BD-empty + AD-empty (negative control), BD-E2 + AD-E2 (control positive) on solid medium synthetic dropout medium without leucine and tryptophan (SD −Leu−Trp) and without histidine (SD −Leu−Trp−His) in the presence of 0, 1, 2.5, 5, and 10 mM 3-amino-1,2,4-triazole (3-AT). **B,** LacZ expression assay in a nitrocellulose membrane. **C,** Schematic representation of the GmβGLU fragment identified in the yeast two-hybrid screen (AD-bbt3, top), and the full-length GmβGLU coding sequence (bottom). The highlighted region represents the region identified in the yeast two-hybrid interaction. SP = signal peptide (1 to 32 amino acids). GH17 = domain of the glycoside hydrolase family 17.

and tan lesions were observed for the susceptible genotype (compatible interaction) and reddish-brown (RB) lesions for the resistant genotype (incompatible interaction). The levels of gene expression in inoculated samples is relative to the levels of transcripts in mock-inoculated samples. In Figure 5, asterisks indicate the means that differ significantly from the mock-inoculated control. In the compatible interaction, GmβGLU mRNA levels were induced at 6, 12, and 24 h postinoculation (hpi), with peak of expression at 12 hpi, as compared with noninoculated plants (Fig. 5A). In the incompatible interaction, GmβGLU expression was induced at 0, 6, 12, 24, 48, and 72 hpi, with peak response at 12 hpi (Fig. 5B). This result demonstrates that the GmβGLU gene is induced in soybean leaves in response to *P. pachyrhizi* in both compatible and incompatible interactions. However, in the compatible interaction, the increased expression is observed only at the beginning of the infection (Fig. 5A). On the other hand, in the incompatible interaction, the gene expression is induced during all analyzed times (Fig. 5B). Still, lower levels of expression were observed in the compatible interaction in comparison to the incompatible interaction.

DISCUSSION

P. pachyrhizi studies related to effectors have mainly been performed based on de novo transcriptome approaches (Carvalho et al. 2017; Elmore et al. 2020; Kunjeti et al. 2016; Link et al. 2014). Recently, the genome of *P. pachyrhizi* Brazilian isolate MT2006 was released to the scientific community by the JGI, which enabled us to identify the gene encoding the de_novo_3939 transcript. We named the effector Phapa-7431740 due to its protein ID in the JGI portal. Our results demonstrated that the de_novo_3939 transcript and its corresponding gene model (Phapa-7431740) were identical (Carvalho et al. 2017). Phapa-7431740 has many features that are consistent with its function as an effector, including the SP, small size, high level of cysteine in its structure (11 residues), and unknown function (Ellis et al. 2009; Petre et al. 2015). The FxC motif present in Phapa-7431740 has been reported as a new class of motifs that is abundant in rust fungi (Germain et al. 2018; Saunders et al. 2012; Zhang et al. 2020). Also, the Y/F/WxC motif has been implicated in translocation of effector proteins across the fungal extrahaustorial membrane (Godfrey et al. 2010).

The Phapa-7431740 gene model also contains a calcium-binding EGF-like domain (EGF_CA). This domain is widely found in nature and regulates several functions, including adhering the proteins to components of the cell matrix, binding to Ca^{2+} ions, and maintaining the function and three-dimensional structure of proteins (Stenflo et al. 2000). In a human pathogen (*Blastomyces dermatitidis)*, the presence of the EGF domain in the BAD1 protein was associated with the pathogenicity of this fungus (Brandhorst et al. 2003, 2005). It will be necessary to investigate the function of the EGF_CA domain in Phapa-7431740, because it may be involved in the pathogenicity of *P. pachyrhizi*.

Our previous work showed that Phapa-7431740 could suppress ETI and induce defense-gene expression (Carvalho et al. 2017). Here, we extended these findings by demonstrating that Phapa-7431740 is also able to suppress the PTI response (Fig. 1). Taken together, our work shows that Phapa-7431740 has functions that are consistent with its potential role as a *P. pachyrhizi* effector. Previous studies reported other rust effector candidates that also have the ability to suppress PTI by reducing ROS production and callose deposition. For example, *Pst_8713* of *Puccinia striiformis* f. sp. *tritici* suppressed callose deposition in wheat leaves after inoculation with EtHAn (Zhao et al. 2018). PSTha5a23 of *P. striiformis* f. sp. *tritici* (Cheng et al. 2017) and 17 *P. pachyrhizi* effector candidates, including PpEC23, were demonstrated to suppress callose deposition (Qi et al. 2016, 2018). A more comprehensive characterization of Phapa-7431740 is an important step to understand how *P. pachyrhizi* suppresses soybean immunity to promote its infection.

We identified GmβGLU as an interactor with Phapa-7431740 by using the yeast two-hybrid assay (Fig. 2). β-1,3-glucanases (E.C. 3.2.1.39) are abundant proteins in plants and have been characterized in many species. These glycoside hydrolase proteins are defined by the GH17 domain and they play fundamental roles in cell division, starch metabolism, cell-wall remodeling, regulation transport through plasmodesmata, and defense against biotic and abiotic stresses (Balasubramanian et al. 2012; Minic 2008; Opassiri et al. 2006; Sekhwal et al. 2013). β-1,3-glucanases are classified as PR-2 proteins that act alone or in association with chitinases (Bertoldo and Mazaro 2018). Therefore, the direct binding of Phapa-7431740 to GmβGLU, a PR-2 protein, suggests that *P. pachyrhizi* can inhibit its activity in order to prevent pathogen recognition by the host or direct action on the fungal cell wall.

Effectors targeting host PR-2 proteins or their transcripts have been described in diverse pathosystems. A microRNA-like sequence (*Pst-milR1*) was described as acting as an effector in *Puccinia striiformis* f. sp. *tritici,* because its transfer to wheat promotes degradation of the β-1,3-glucanase (*SM638*) transcript by the host RNA silencing machinery (Wang et al. 2017). A nematode effector targets the *Arabidopsis* PR-2 protein to control callose formation or limit the generation of defense signaling molecules (Hamamouch et al. 2012). Finally, in a viral system, the P3 movement protein of soybean mosaic virus was demonstrated to interact with an endo-1,3-β-glucanase to promote virus pathogenicity (Shi et al. 2020). These examples demonstrate

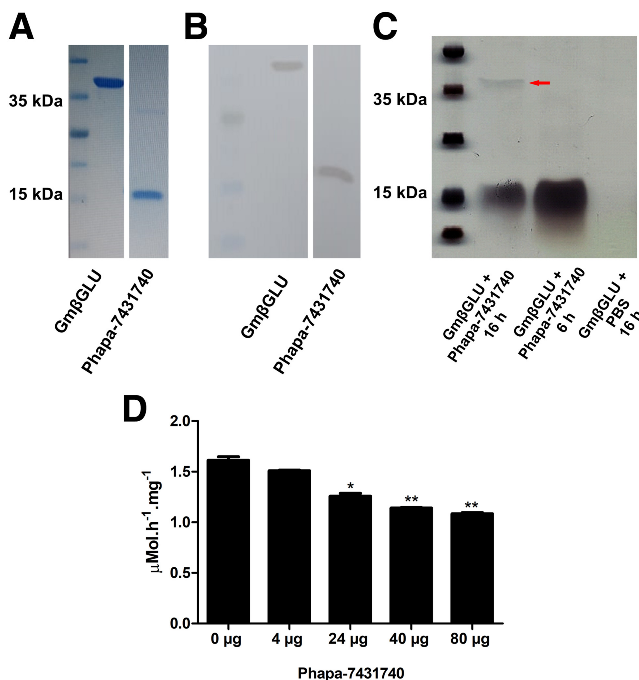

Fig. 3. In vitro validation of the GmβGLU and Phapa-7431740 interaction. **A,** Sodium dodecyl sulfate-polyacrylamide gel electrophoresis of proteins purified by fast protein liquid chromatography. **B,** Western blot to detect purified proteins using an anti–HIS-tag antibody. **C,** Phapa-7431740 and GmβGLU interact in a pull-down assay. GmβGLU was incubated with Phapa-7431740 beads for 16 (left lane) or 6 h (middle lane) and with empty beads for 16 h (right lane, negative control). The red arrow indicates the GmβGLU band. **D,** Phapa-7431740 inhibits GmβGLU activity in a dose-dependent manner. One asterisk (*) indicates significance at $P < 0.05$ and two (**) indicate significance at $P < 0.01$, as determined by the *t* test.

that PR-2 proteins are broadly targeted by pathogen effectors. Therefore, it is no surprise that soybean rust may deploy effectors that target members of this host protein family to promote infection.

We demonstrated that Phapa-7431740 inhibited GmβGLU activity in vitro with a dose-dependent manner (Fig. 3D). Thus, the evidence shows that Phapa-7431740 is able to directly inhibit the activity of GmβGLU in vitro. In the *Fusarium verticillioides*–maize pathosystem, *F. verticillioides* produces a toxin, fumonisin B1, that suppresses the activity of β-1,3-glucanases. An activity assay using purified FB1 showed that it inhibited the basic β-1,3-glucanases in a dose-dependent manner, similar to Phapa-7431740 in our work (Sánchez-Rangel et al. 2012). In soybean, the glucanase inhibitor protein 1 (GIP1) effector of *Phytophthora sojae* interacts specifically with soybean endo-β-1,3-glucanase A (*EGaseA*) to inhibit its activity (Bishop et al. 2005).

Expression profiling during the compatible interaction showed *GmβGLU* mRNA transcripts were induced early in the infection process at 6, 12, and 24 hpi (Fig. 5A). In the first 12 hpi, most of the germinated urediniospores have already formed the appressorium and are in the process of penetrating epidermal cells (Schneider et al. 2011). Interestingly, we previously showed that *Phapa-7431740* transcript was also induced in *P. pachyrhizi* at these times in a susceptible soybean genotype (BRS 231) inoculated with *P. pachyrhizi* (Carvalho et al. 2017). The expression of *Phapa-7431740* and *GmβGLU* at the same time periods further suggests that interaction between them is possible and it occurs from the beginning of the infection, possibly preventing GmβGLU from degrading the pathogen cell wall.

The induction of GmβGLU expression at the beginning of infection indicates that it is deployed early in defense against the fungus. β-1,3-Glucanases hydrolyze and release β-D-glucans from the fungal cell well to damage them. The released β-D-glucans can act as defense inducers in the plant by eliciting accumulation of phytoalexins and other PTI responses (Edreva 2004; Klarzynski et al. 2000; Okinaka et al. 1995; Simões et al. 2005). Therefore, GmβGLU may be induced at the beginning of the infection to not only directly damage the invader but, also, to assist in pathogen recognition and activation of plant defense responses. Inhibiting the activation of plant defenses is

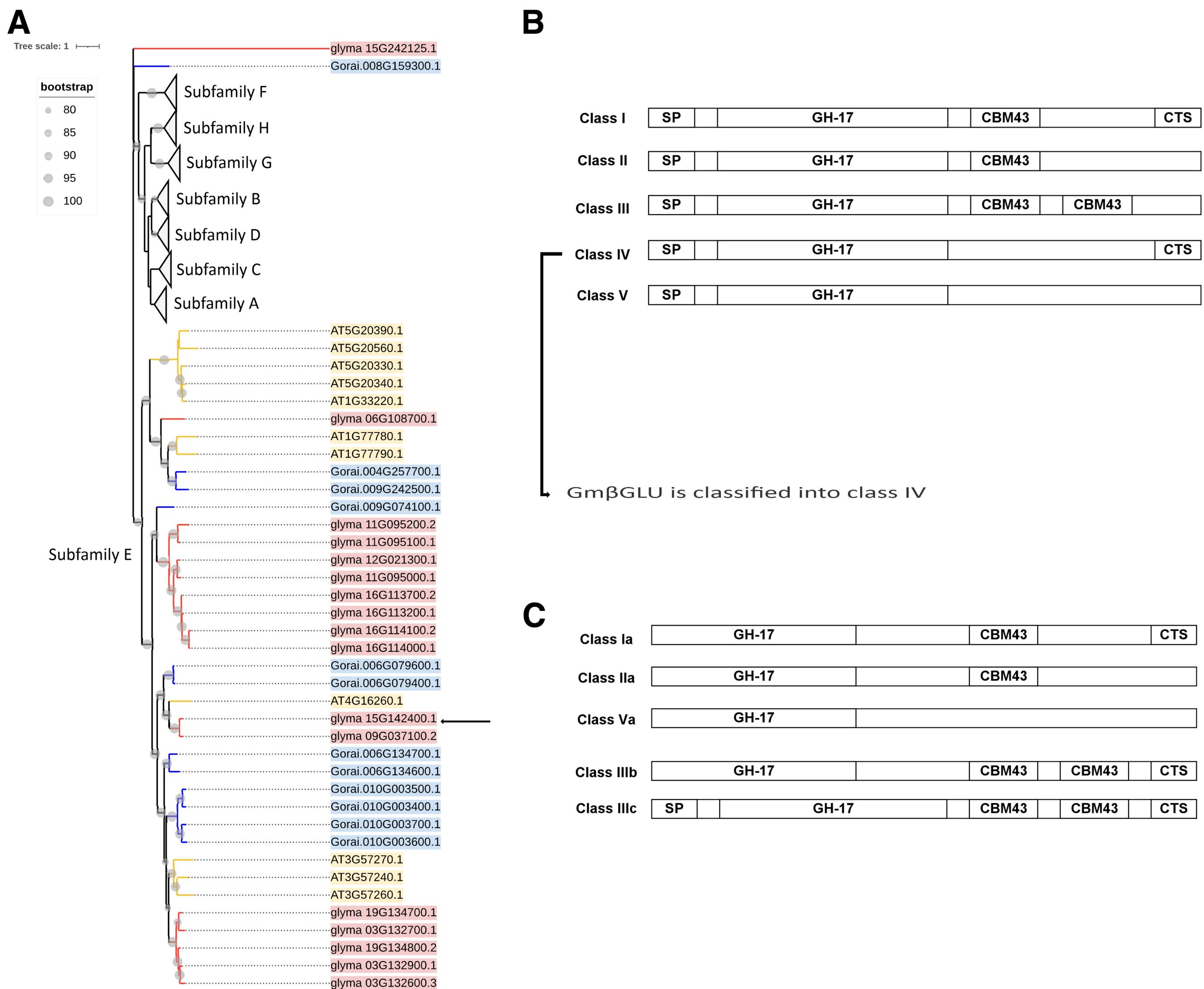

Fig. 4. Phylogenetic tree of PR-2 family members in *Glycine max*, *Gossypium raimondii*, and *Arabidopsis thaliana* and the protein domain architectures of β-1,3-glucanases. **A,** The phylogenetic tree was divided into eight subfamilies (subfamilies A through H) and only subfamily E members are expanded in the tree. The arrow indicates the location of the soybean GmβGLU that interacts with Phapa-7431740. **B,** Five classes based on the presence or absence and number of CBM43 and C-terminal sequence (CTS) domains in the C-terminal region. **C,** Structural variations of classes I, II, III, and V observed in the soybean protein sequences. SP = signal peptide; GH-17 = glycoside hydrolase domain of family 17; CBM43 = carbohydrate binding module of family 43.

consistent with our observation that Phapa-7431740 suppresses defense responses associated with PTI.

In the incompatible interaction, the expression profile of GmβGLU was different from the compatible interaction in that its expression was induced at all times and at higher levels throughout the infection time course (Fig. 5B). We hypothesize that initially GmβGLU is expressed as part of a general response to *P. pachyrhizi*. However, subsequent recognition by the resistance gene causes GmβGLU expression to become elevated and maintained during the incompatible soybean–*P. pachyrhizi* interaction. The *PR-2* gene is associated with a basal nonspecific resistance against *P. pachyrhizi* in soybean, therefore, enhancing specific resistance conferred by single dominant *Rpp* genes. A recent study mapped seven putative resistance (*R*) genes surrounded by seven putative glucan endo-1,3-β-glucosidases upstream of the *R*-gene locus for hop resistance to powdery mildew caused by *Podosphaera humuli*, indicating a physical link of among these genes. In this study, RNA-Seq data showed all putative *R* genes along with all putative glucan endo-1,3-β-glucosidase genes were expressed under diseased conditions

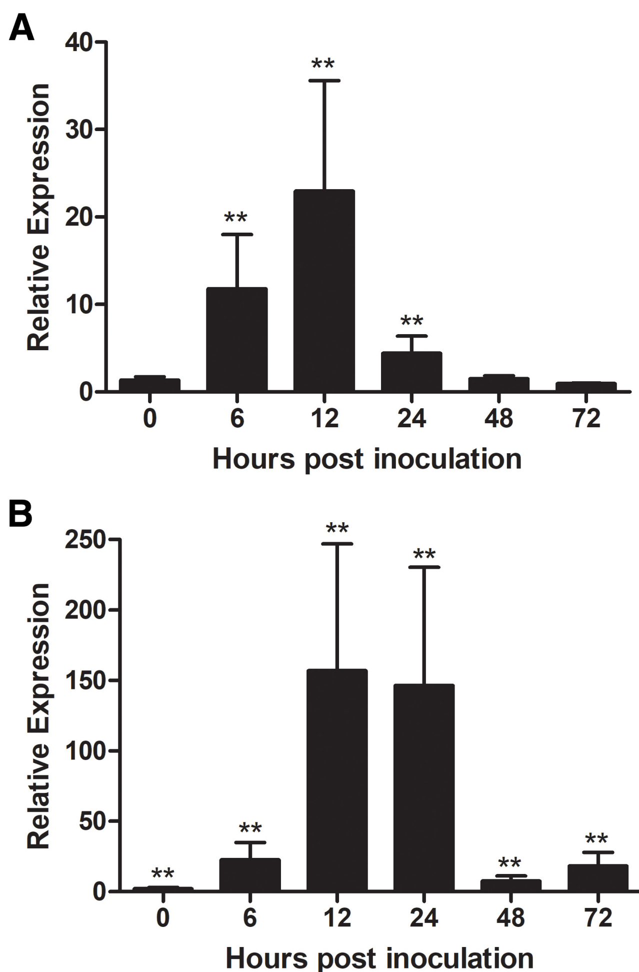

Fig. 5. Relative expression of GmβGLU in susceptible and resistant soybean lines over a 72-h time course after inoculation. **A,** Relative expression of GmβGLU in the susceptible soybean genotype (cultivar BRS 184). **B,** Relative expression of GmβGLU in the resistant soybean genotype (Rpp5). The endogenous genes EF1β and TUA-4 were used as normalizers and plants not inoculated with the fungus isolate were used as calibrator. The levels of gene expression in the inoculated samples is relative to the levels of transcripts in the mock-inoculated samples. The asterisk indicates the means that differ significantly from the mock-inoculated control. Two asterisks (**) indicate significance at $P < 0.01$, as determined by the pair-wise fixed reallocation randomization test.

(Padgitt-Cobb et al. 2020). Another study reporting the identification of the wheat stem rust resistance gene *Sr21* (coiled-coil nucleotide-binding leucine-rich repeat protein) also demonstrated a coordinated upregulation of six *PR* genes (including a *PR-2*) triggered by *Sr21* (Chen et al. 2018). Thus, we wonder whether a similar coordination may be occurring in the *P. pachyrhizi*–soybean pathosystem.

The β-1,3-glucanases comprise complex and diverse families in plants that act in a variety of developmental and physiological processes (Doxey et al. 2007). Due to this complexity and diversity, a comparative analysis of the β-1,3-glucanases proteins of soybean was performed with homologous proteins found in cotton (*Gossypium raimondii*) (Xu et al. 2016) and *Arabidopsis* (Doxey et al. 2007). β-1,3-Glucanases are members of the PR-2 family, which have the GH17 domain as their predominant structural feature (Henrissat 1991; Kitajima and Sato 1999; Yamaguchi et al. 2002; Zavaliev et al. 2013).

Previous studies have sought to characterize the β-1,3-glucanases in soybean. The first one, described only 12 β-1,3-glucanases, of which four were placed into tobacco class I, five into classes II and IV, two into class V, and one into class III (Jin et al. 1999). In another study using *PR* gene sequences as queries in tBLASTn searches against the soybean transcriptome, 310 *PR* genes were identified, with *PR-2* genes being one of the most highly represented (Wanderley-Nogueira et al. 2012). However, neither of these studies used the soybean reference genome as a basis for the analyses.

Our analysis identified 91 soybean PR-2 family members in the soybean reference genome that were divided into eight subfamilies (Fig. 4A). The GmβGLU protein was classified in subfamily E, together with the *EGaseA* protein, which is the *Phytophthora sojae* GIP effector target (Bishop et al. 2005). This *PR-2* gene, encoded by the gene model Glyma.19G134700.1, was also previously reported as important in plant development and defense against pathogens (Cheong et al. 2000).

There are few additional studies related to the functions of the *PR-2* genes in soybean, and the majority of these have investigated the function of Glyma.03G132700 against pathogens. In one study, the ethylene-responsive element-binding protein (EREBP) transcription factor (named as *GmEREBP1*) was associated with resistance to soybean cyst nematode because its transcript abundance increased in the infected roots of a resistant cultivar (Mazarei et al. 2002). Transgenic soybean plants overexpressing *GmEREBP1* activated the expression of the ethylene-responsive *PR-2* gene (Mazarei et al. 2007). Furthermore, the mRNA expression of this *PR-2* gene was also induced upon infestation by the soybean aphid *Aphis glycines* Matsumura (Zhong et al. 2014) and the root-infecting *Fusarium virguliforme* (Abdelsamad et al. 2019). Interestingly, this *PR-2* gene (Glyma.03G132700) was classified in subfamily E.

In addition, subfamily E members from other species have been described as related to disease resistance. The *Arabidopsis* protein sequences AT3G57270, AT3G57260, AT3G57240, and AT4G16260 share more than 50% identity with GmβGLU. These mRNA transcripts encoding these secreted PR-2 proteins are induced during infection by bacterial and fungal pathogens (Dong et al. 1991; Doxey et al. 2007). The AT4G16260 protein interacts with the beet cyst nematode effector (30C02) and, when AT4G16260 is overexpressed in *Arabidopsis* roots, beet cyst nematode infection is significantly reduced (Hamamouch et al. 2012).

While Phapa-7431740 was found to interact with GmβGLU (Glyma.15G142400), alignment of the amino acid sequences corresponding to the region identified in the yeast two-hybrid interaction among the 15 soybean subfamily E members demonstrated that there is more than 59% identity (Table 1). Moreover, Glyma.09G037100.4 is most similar, with 88% identity to

the region. The similarity of the sequences suggests that Phapa-7431740 may be able to interact with multiple soybean subfamily E members and further studies are needed to test this hypothesis.

In conclusion, our results suggest that Phapa-7431740 may function as a *P. pachyrhizi* effector that interferes with PTI by controlling β-1,3-glucanase activity, suggesting that inhibition of PTI is necessary for successful infection of soybean. Our study further indicates an important role for PR-2 proteins in the basal defense of soybean against *P. pachyrhizi*.

MATERIALS AND METHODS

In silico identification of the effector candidate Phapa-7431740.

The transcript sequence of the *P. pachyrhizi* effector candidate de_novo_3939 (Carvalho et al. 2017) was analyzed for significant similarity (70% identity and 50% coverage) with the protein sequences of the reference genome from *P. pachyrhizi* (MT2006) available at the JGI MycoCosm database (accessed November 17, 2021). Phapa-7431740 was selected as the gene model with highest similarity to de_novo_3939. For protein characterization, the number and percentage of cysteine residues in the mature protein and presence of domains conserved by PFAM were determined. Domains with E-values greater than 10^{-5} were ignored (Saunders et al. 2012).

PTI suppression.

N. benthamiana plants were grown in a growth chamber at 24°C with a 12-h photoperiod. The Phapa-7431740 coding sequence was cloned into *Pseudomonas fluorescens* Pf0-1 (EtHAn) using the pEDV6 plasmid (Sohn et al. 2007). Recombinant EtHAn bacteria were grown in Kings B (KB) medium with 30 μg of chloramphenicol and 50 μg of gentamicin per milliliter for 48 h at 28°C. Bacterial colonies were resuspended with water and were centrifuged at 3,000 × *g* for 15 min, the pellets were resuspended in 2 ml of infiltration solution (10 mM $MgCl_2$) and were adjusted to an optical density measured at 600 nm (OD_{600}) equal to 0.5. The bacterial suspensions were infiltrated into the abaxial surface of leaves of 5-week-old *N. benthamiana* plants, using a needleless syringe. As negative control, *N. benthamiana* leaves were infiltrated with the $MgCl_2$ solution, and, as a positive control, leaves were infiltrated with EtHAn containing the pEDV6 empty vector. The experiment was conducted with nine replicates, with one plant per replicate in a completely randomized design experiment. After infiltration, all strains used in the bioassay were recovered from the inoculation site 48 h after infiltration, were grown in KB medium, and the colonies were used in a PCR assay to demonstrate that the recovered strain was the same strain we have inoculated (data not presented).

N. benthamiana infiltrated leaves were used for ROS detection and callose deposition analysis. At 24 h postinfiltration, leaf discs were collected for the analysis of ROS. The leaf discs were stained overnight with 3,3′′-diaminobenzidine under gentle stirring at room temperature. The leaf discs were washed with distilled water, were de-stained for 15 min with a warmed solution of ethanol/glycerol/acetic acid (3:1:1), and were mounted in 50 % glycerol. Images were acquired using the Motic Images Plus 2.0 software.

To test the callose deposition in *N. benthamiana* leaves, leaf discs were collected 72 h postinfiltration. Leaf discs were de-stained overnight in 95% ethanol under agitation at 37°C, followed by several successive washes with 70% ethanol. Leaf discs were stained with a solution of aniline blue (150 mM potassium phosphate, pH 9.0) for 1 h, under agitation in the dark at room temperature. Excess dye was removed by washing in water, leaf discs were examined using a fluorescent microscope, and the images were analyzed using the Zeiss AxioVision 3.0 software.

The ROS images were taken on the 10× objective lens and callose deposition images were taken on the 5× objective lens. These images were acquired avoiding the edges of the leaf discs that suffer greater stress, focusing on the central region, so that in the upper left corner is the region of the infiltration point. ROS and callose deposition values were obtained by quantification of image pixels. The values obtained in the negative control ($MgCl_2$ solution) were used as a calibrator in the calculations that generated the graphs. Statistical differences following image analysis were performed using the *t* test.

Yeast two-hybrid assay.

Phapa-7431740 gene model cloning. The Phapa-7431740 coding sequence was amplified with specific primers (Supplementary Table S1) and was cloned into the vector pCR8/GW/TOPO (Invitrogen), forming the entry vector GW/TOPO_Phapa-7431740. After sequence confirmation, LR clonase (Invitrogen) was used to transfer the Phapa-7431740 coding sequence to pDEST32 (LEU2, CEN, gentamicin), forming the vector BD-7431740, which was confirmed by sequencing. The BD-7431740 clone fused Phapa-7431740 to the DNA binding domain (BD) of Gal4p.

Transactivation assay. A preliminary transactivation assay was performed to confirm that Phapa-7431740 did not activate the reporter system alone. The yeast *Saccharomyces cerevisiae* AH109 (MATa, trp1-901, leu2-3,112, ura3-52, his3-200, gal4Δ, gal80Δ, LYS2::GAL1UAS-GAL1TATA-HIS3, GAL2 UASGAL2TATA-ADE2, URA3::MELUAS-MEL1TATAlacZ)

Table 1. Soybean proteins of subfamily E in relation to the region identified in the GmβGLU protein

Gene name	Identity (%)	Coverage (%)	Protein size (aa)	E-VALUE
Glyma.09G037100.4	88	100	371	$1.0E^{-61}$
Glyma.19G134800.2	62	74	347	$1.0E^{-35}$
Glyma.03G132700.1	61	74	348	$7.0E^{-34}$
Glyma.06G108700.1	45	74	341	$4.0E^{-19}$
Glyma.11G095100.1	64	72	345	$3.0E^{-34}$
Glyma.12G021300.1	56	72	327	$2.0E^{-31}$
Glyma.11G095000.1	55	72	339	$1.0E^{-27}$
Glyma.19G134700.1	63	70	349	$4.0E^{-33}$
Glyma.03G132900.1	64	69	341	$7.0E^{-35}$
Glyma.16G113200.1	60	69	332	$3.0E^{-31}$
Glyma.16G113700.2	59	69	275	$1.0E^{-30}$
Glyma.16G114100.2	59	69	335	$6.0E^{-30}$
Glyma.16G114000.1	59	69	335	$6.0E^{-30}$
Glyma.11G095200.2	59	65	237	$7.0E^{-27}$

was transformed using the lithium acetate and polyethylene glycol (PEG) method, with the BD-7431740 vector (bait) and the pDEST22 vector empty. The transformants were plated on SD selection medium without leucine and tryptophan (SD −LEU−TRP). The transformed AH109 colonies grown in liquid were used in the HIS3 reporter gene transactivation assay, according to the Clontech manual, with varying 3-AT concentrations. The result of this assay was used to determine the inhibitor concentration to be used in the screening.

Screening for Phapa-7431740-interacting soybean proteins. The yeast two-hybrid screen was performed according to the Clontech manual, with a previously prepared cDNA library (Alves et al. 2011). AH109 carrying BD-7431740 were inoculated in SD −LEU medium and were grown for 16 to 18 h at 28°C and 180 rpm. The pre-inoculum was transferred to 80 ml of SD −LEU medium and was maintained at 28°C and 180 rpm until an $OD_{600} = 0.4$ to 0.6 was reached. The culture was centrifuged at 5,000 × *g* for 10 min, and the pellet was resuspended in autoclaved distilled water. The washing step was repeated three times. In the final wash, the pellet was resuspended in the transformation mix (7.2 ml of 50% PEG (mass/volume), 1.08 ml of 1 M lithium acetate, 1.5 ml of DNA salmon sperm single strand DNA previously boiled for 5 min, and 1.02 ml of DNA (20 μl of soybean cDNA library + 1 ml of water) and was maintained at 42°C for 50 min. The transformation was centrifuged at 5,000 × *g* at 20°C for 10 min, and the pellet was washed three times with distilled water and was resuspended in SD −LEU−TRP−HIS. The transformation was plated in SD −LEU−TRP−HIS medium.

Colonies were transferred to plates with SD −LEU−TRP−HIS selection medium at concentrations 0.0, 1.0, 2.5, 5.0, and 10.0 mM 3-AT. Colonies grown in the highest concentration of 3-AT were transferred to liquid selection medium, and the plasmids were extracted with the Zymoprep yeast plasmid miniprep I kit (Zymo Research) and were then transformed into DH5α *E. coli*.

Characterization of interactions by activating reporter genes. Interactions were characterized, based on activation of two reporter genes, according to guidelines in the Clontech manual. The first of these reporter genes, *HIS3*, encodes the imidazolglycerol phosphate dehydratase (EC 4.2.1.19) enzyme (His3p). This enzyme has a competitive inhibitor, 3-AT. For this assay, the yeast clones obtained in the screening were plated in selective SD −LEU−TRP−HIS media with different concentrations of 3-AT, ranging from 0 to 10 mM, and were grown in a biochemistry oxygen demand incubator at 28°C for 7 days.

The second reporter gene, *LacZ*, encodes the β-galactosidase enzyme (EC 3.2.1.23), and the activity of this gene can be visualized by the degradation of 5-bromine-4-chlorine-3-indoxyl-β-D-galactopyranoside (X-gal), which results in the appearance of blue staining. In this assay, the yeast clones were transferred to a nitrocellulose membrane placed on SD −LEU −TRP solid medium and were grown at 28°C for 4 days. After the yeast growth, the membrane was submerged in liquid nitrogen to rupture the yeast cells and, then, was placed on filter paper soaked in Z buffer (60 mM Na_2HPO_4, 40 mM NaH_2PO_4, 10 mM KCl, 1 mM $MgSO_4$, pH 7.0) added with X-gal (0.5 mg ml^{-1}). The membrane was incubated at 28°C until a blue color developed.

For both assays, the GmbZIPE2 protein (BD-E2 + AD-E2) was used as a positive control (Alves et al. 2015). The negative controls were the empty plasmids (BD-empty + AD-empty) and the plasmid BD containing the Phapa-7431740 effector together with the empty plasmid AD (BD-7431740 + AD-empty).

Analysis of prey sequences. The prey sequences were amplified with primers based on the pEXP-AD-502 vector (Supplementary Table S1), and the PCR amplicons were sequenced by Sanger sequencing. The sequences were trimmed by removing the pEXP-AD-502 vector and subsequently analyzed in ORFINDER to identify the open reading frames. The sequences were analyzed for similarity to corresponding soybean proteins using Phytozome and National Center for Biotechnology Information (NCBI) databases.

Heterologous expression and protein purification.

The gene models Phapa-7431740 and Glyma.15G142400 (GmβGLU) were synthesized in the pET28a expression vector by Biomatik. The gene sequences without the SP were optimized to heterologous expression in *E. coli*. The construction allows the fusion of a His-tag in the N-terminal region of the protein.

Expression of Phapa-7431740 in E. coli *BL21 (DE3)-pRare. E. coli* BL21 (DE3)-pRare was grown in a selective medium supplemented with 50 μg of chloramphenicol per milliliter and was cultured for 12 h in a 37°C shaking incubator at 180 rpm. The bacteria were transformed with the pET28a-Phapa-7431740 vector using a $CaCl_2$-mediated transformation method. The transformants were confirmed by colony PCR using specific primers (Supplementary Table S1).

The transformed colony was cultivated in Luria Bertani (LB) medium containing 50 μg of kanamycin and 50 μg of chloramphenicol per milliliter. The pre-inoculum was transferred to a 1,000-ml LB medium and cultivated at 37°C until OD_{600} reached 0.6. Expression of the protein was induced by the addition of 0.4 mM isopropyl β-D-1-thiogalactopyranoside (IPTG) for4 h at 37°C.

GmβGLU protein expression in ArcticExpress (D3). ArcticExpress (D3) cells were transformed with the pET28a-GmβGLU vector as described above and were grown in LB medium supplemented with 50 μg of kanamycin and 35 μg of gentamicin per milliliter. After overnight incubation at 37°C, the pre-inoculum was transferred to a 1,000-ml LB medium and was cultured at 30°C until the OD_{600} reached 0.6. Protein expression was induced with 0.4 mM IPTG for 24 h at 12°C.

Protein extraction and purification. The induced cells were harvested by centrifugation at 3,000 × *g* and were suspended with a ligation buffer (20 mM Na_2HPO_4, 500 mM NaCl, 20 mM imidazole, pH 7.4). For total protein extraction, the suspension was subjected to sonication for 5 min in 30-s bursts, amplitude 40, and 30-s interval between two successive pulses. Soluble extracts were obtained from the supernatants recovered after centrifugation at 10,000 × *g* for 20 min at 4°C. The soluble fractions of both proteins were purified by affinity chromatography in a HisTrap 1-ml column, using the AKTA fast protein liquid chromatography system. The protein profile of the extraction and purification were analyzed by SDS-PAGE and Western blot, using an anti-His monoclonal antibody (Invitrogen) (Liao et al. 2008).

Pull-down assay.

The interaction between GmβGLU and Phapa-7431740 was evaluated by pull-down assay. The treatments were GmβGLU with effector (40 μg of both proteins) and GmβGLU without effector (GmβGLU + phosphate-buffered saline [PBS]) negative control. Primarily, the Phapa-7431740 was incubated with the beads (Pierce NHS-activated magnetic beads) at 12°C for 6 h with agitation. The negative control was incubated at the same conditions with PBS. Next, the samples were washed three times and the beads were incubated with a quenching buffer (3 M ethanolamine, pH 9.0) for 16 h of agitation. The beads were incubated with GmβGLU at 12°C for two lengths of time (6 and 16 h) with agitation. The interaction was permitted in the presence of 1mM $CaCl_2$. Finally, the beads were washed three times with PBS. The proteins present in the pull-down assay were detected by SDS-PAGE and silver staining. The interaction was confirmed by the presence of two bands in the same lane.

Enzymatic activity.

Free glucose was quantified by 3,5-dinitrosalicylic acid assay (DNS). The assay consisted of two technical replicates and was performed three independent times. The treatments were GmβGLU with effector (4, 24, 40, or 80 μg of effector protein), GmβGLU without effector (40 μg protein), and negative control (40 μg of the GmβGLU after stopped reaction with DNS reagent). In addition to these treatments, the assay was performed in the same way using an unrelated protein (BSA) as a control.

Proteins were incubated at 12°C for 16 h with agitation. The interaction occurred in the presence of 1 mM $CaCl_2$. After incubation, the following reactions were prepared: 140 μl of proteins, 125 μl of 2–mg ml^{-1} laminarin, 1.3 μl of 0.1 M $CaCl_2$, 233.7 μl of 50 mM calcium acetate, pH 5. Reactions were incubated at 37°C for 9 h and were then stopped by adding 500 μl of the DNS reagent. The solutions were boiled for 5 min, and the absorbance was then measured at 540 nm. The enzyme activity (micromole per hour per milligram) was calculated based on a standard curve prepared using glucose, the time of reaction, and the protein concentration.

***In silico* characterization of the PR-2 family in soybean.**

To identify soybean PR-2 family proteins, similarity searches were initially performed using the program HMMSEARCH (HMMER package) (Eddy 2011) and the PFAM model (El-Gebali et al. 2019) PF00332 (GH17). To determine if any unrelated sequence was selected, similarity searches using the BLASTp program against the NCBI nonredundant database were performed using the E-value cutoff of $<10^{-5}$.

For comparative analysis of PR-2 family proteins, a multiple sequence alignment (MSA) was constructed using the selected soybean sequences together with cotton (*Gossypium raimondii*) (Xu et al. 2016) and *A. thaliana* (Doxey et al. 2007) PR-2 sequences using the MUSCLE program (Edgar 2004) with default parameters. The complete protein sequences were used to do the alignment. The resulting MSA was used to build a phylogenetic tree with the IQ-TREE program (Minh et al. 2020), also using default parameters. To classify selected soybean proteins according to their domain structure, a set of *in silico* analyses was performed. First, to identify the NTS, the SignalP program (versions 3 and 5) (Nielsen et al. 1997) was used. In order to define which sequences possess the X8 domain (CBM43), similarity searches of the PFAM model PF07983 (X8 domain) against the soybean proteins were performed using HMMSEARCH program. Finally, to check for the presence of the hydrophobic CTS, the PredGPI (Pierleoni et al. 2008) and deepLoc (Almagro Armenteros et al. 2017) programs were used to identify the presence of the GPI anchor and vacuolar signal sequence, respectively.

Expression profile of GmβGLU during an infection time course.

The expression profile of GmβGLU was analyzed during the infectious cycle in susceptible soybean genotypes (BRS184) and a resistant genotype carrying *Rpp5*. The LPF16.1M pure isolate was used to inoculate both genotypes. The experiment was performed in a completely randomized design with three replications. The soybean plants were grown in 0.5-liter plastic pots and were kept in a climatic growth chamber (Fitotron). When the plants reached the V_3 stage, the rust isolate was inoculated on the first and second trifoliate leaves of each plant. The leaves were collected at 0, 6, 12, 24, 48, and 72 hpi.

Total RNA extraction and cDNA synthesis. The inoculated and noninoculated soybean leaves (mock) were macerated with liquid nitrogen and the total RNA was extracted by the Trizol method (Invitrogen), according to manufacturer protocol. The RNA was resuspended in 35 μl of ultrapure water and was stored at −80°C. RNA concentrations were quantified on a NanoDrop 1000 spectrophotometer (Thermo Scientific) and the integrity was analyzed on 1% agarose gel. To eliminate the genomic DNA, 5 μg of RNA was treated with DNase I (Invitrogen) and was visualized on a 1% agarose gel to confirm the efficiency of the treatment. Subsequently, cDNA was synthesized using the SuperScript III first-strand kit (Invitrogen), following manufacturer instructions. Amplification of the cDNA was confirmed and the cDNA was stored at −20°C.

RT-qPCR analysis. The primers for the GmβGLU gene were designed using Primer3Plus (Supplementary Table S1), and the efficiency of each primer-pair was determined using serial cDNA dilutions and calculating the linear regression obtained for each gene. The expression profile was monitored by qPCR, using elongation factor 1 β (*EF-1*β) (Hu et al. 2009) and α-tubulin (*TUA 4*) (Ma et al. 2013) as normalizing genes, and noninoculated plants were used as a calibrator. The amplification conditions were 95°C for 10 min, 40 cycles of 94°C for 15 s, and 60°C for 1 min, followed by melting curve analysis. qPCR was performed on the 7900HT fast real-time PCR system (Applied Biosystems), using the Platinum SYBR Green qPCR SuperMix-UDG kit (Invitrogen). The samples were analyzed in two independent runs and each PCR reaction was performed in triplicate. The expression levels of the target genes were determined by relative quantification, using the REST software (Pfaffl et al. 2002).

AUTHOR-RECOMMENDED INTERNET RESOURCES

JGI Phytozome database: https://phytozome.jgi.doe.gov
JGI MycoCosm database:
https://mycocosm.jgi.doe.gov/pages/blast-query.jsf?db=Phapa1
NCBI BLAST search tool: http://blast.ncbi.nlm.nih.gov
ORFINDER: http://www.ncbi.nlm.nih.gov/gorf/gorf.html

LITERATURE CITED

Abdelsamad, N. A., MacIntosh, G. C., and Leandro, L. F. S. 2019. Induction of ethylene inhibits development of soybean sudden death syndrome by inducing defense-related genes and reducing *Fusarium virguliforme* growth. PLoS One 14:e0215653.

Aime, M. C., McTaggart, A. R., Mondo, S. J., and Duplessis, S. 2017. Phylogenetics and phylogenomics of rust fungi. Adv. Genet. 100: 267-307.

Almagro Armenteros, J. J., Sønderby, C. K., Sønderby, S. K., Nielsen, H., and Winther, O. 2017. DeepLoc: Prediction of protein subcellular localization using deep learning. Bioinformatics 33:3387-3395.

Alves, M. S., Reis, P. A. B., Dadalto, S. P., Faria, J. A. Q. A., Fontes, E. P. B., and Fietto, L. G. 2011. A novel transcription factor, ERD15 (Early Responsive to Dehydration 15), connects endoplasmic reticulum stress with an osmotic stress-induced cell death signal. J. Biol. Chem. 286:20020-20030.

Alves, M. S., Soares, Z. G., Vidigal, P. M. P., Barros, E. G., Poddanosqui, A. M. P., Aoyagi, L. N., Abdelnoor, R. V., Marcelino-Guimarães, F. C., and Fietto, L. G. 2015. Differential expression of four soybean bZIP genes during *Phakopsora pachyrhizi* infection. Funct. Integr. Genomics 15:685-696.

Balasubramanian, V., Vashisht, D., Cletus, J., and Sakthivel, N. 2012. Plant β-1,3-glucanases: Their biological functions and transgenic expression against phytopathogenic fungi. Biotechnol. Lett. 34:1983-1990.

Barral, P., Suárez, C., Batanero, E., Alfonso, C., Alché, Jde D., Rodríguez-García, M. I., Villalba, M., Rivas, G., and Rodríguez, R. 2005. An olive pollen protein with allergenic activity, Ole e 10, defines a novel family of carbohydrate-binding modules and is potentially implicated in pollen germination. Biochem. J. 390:77-84.

Benson, D. A., Clark, K., Karsch-Mizrachi, I., Lipman, D. J., Ostell, J., and Sayers, E. W. 2014. GenBank. Nucleic Acids Res. 42:D32-D37.

Bertoldo, É., and Mazaro, S. M. 2018. β-1,3 Glucanases: Uma revisão sob a ótica da defesa vegetal. Sci. Agrar. Parana. 17:1-13.

Bishop, J. G., Ripoll, D. R., Bashir, S., Damasceno, C. M. B., Seeds, J. D., and Rose, J. K. C. 2005. Selection on glycine β-1,3-endoglucanase genes differentially inhibited by a Phytophthora glucanase inhibitor protein. Genetics 169:1009-1019.

Borner, G. H. H., Sherrier, D. J., Stevens, T. J., Arkin, I. T., and Dupree, P. 2002. Prediction of glycosylphosphatidylinositol-anchored proteins in Arabidopsis. A genomic analysis. Plant Physiol. 129:486-499.

Brandhorst, T., Gauthier, G. M., Stein, R. A., and Klein, B. S. 2005. Calcium binding by the essential virulence factor BAD-1 of *Blastomyces dermatitidis*. J. Biol. Chem. 280:42156-42163.

Brandhorst, T., Wüthrich, M., Finkel-Jimenez, B., and Klein, B. 2003. A C-terminal EGF-like domain governs BAD1 localization to the yeast surface and fungal adherence to phagocytes, but is dispensable in immune modulation and pathogenicity of *Blastomyces dermatitidis*. Mol. Microbiol. 48:53-65.

Bromfield, K. R., and Hartwig, E. E. 1980. Resistance to soybean rust and mode of inheritance. Crop Sci. 20:254-255.

Carvalho, M. C. da C. G., Costa Nascimento L., Darben L. M., Polizel-Podanosqui, A. M., Lopes-Caitar, V. S., Qi, M., Rocha, C. S., Carazzolle, M. F., Kuwahara, M. K., Pereira, G. A. G., Abdelnoor, R. V., Whitham, S. A., and Marcelino-Guimarães, F. C. 2017. Prediction of the in planta *Phakopsora pachyrhizi* secretome and potential effector families. Mol. Plant Pathol. 18:363-377.

Chang, J. H., Urbach, J. M., Law, T. F., Arnold, L. W., Hu, A., Gombar, S., Grant, S. R., Ausubel, F. M., and Dangl, J. L. 2005. A high-throughput, near-saturating screen for type III effector genes from *Pseudomonas syringae*. Proc. Natl. Acad. Sci. U. S. A. 102:2549-2554.

Chen, S., Zhang, W., Bolus, S., Rouse, M. N., and Dubcovsky, J. 2018. Identification and characterization of wheat stem rust resistance gene *Sr21* effective against the Ug99 race group at high temperature. PLoS Genet. 14:1-21.

Cheng, Y., Wu, K., Yao, J., Li, S., Wang, X., Huang, L., and Kang, Z. 2017. PSTha5a23, a candidate effector from the obligate biotrophic pathogen *Puccinia striiformis* f. sp. *tritici*, is involved in plant defense suppression and rust pathogenicity. Environ. Microbiol. 19:1717-1729.

Cheong, Y. H., Kim, C. Y., Chun, H. J., Moon, B. C., Park, H. C., Kim, J. K., Lee, S.-H., Han, C., Lee, S. Y., and Cho, M. J. 2000. Molecular cloning of a soybean class III β-1,3-glucanase gene that is regulated both developmentally and in response to pathogen infection. Plant Sci. 154: 71-81.

Childs, S. P., King, Z. R., Walker, D. R., Harris, D. K., Pedley, K. F., Buck, J. W., Boerma, H. R., and Li, Z. 2018. Discovery of a seventh Rpp soybean rust resistance locus in soybean accession PI 605823. Theor. Appl. Genet. 131:27-41.

Dong, X., Mindrinos, M., Davis, K. R., and Ausubel, F. M. 1991. Induction of *Arabidopsis* defense genes by virulent and avirulent *Pseudomonas syringae* strains and by a cloned avirulence gene. Plant Cell 3:61-72.

Doxey, A. C., Yaish, M. W. F., Moffatt, B. A., Griffith, M., and McConkey, B. J. 2007. Functional divergence in the *Arabidopsis* β-1,3-glucanase gene family inferred by phylogenetic reconstruction of expression states. Mol. Biol. Evol. 24:1045-1055.

Eddy, S. R. 2011. Accelerated profile HMM searches. PLoS Comput. Biol. 7:e1002195.

Edgar, R. C. 2004. MUSCLE: Multiple sequence alignment with high accuracy and high throughput. Nucleic Acids Res. 32:1792-1797.

Edreva, A. 2004. A novel strategy for plant protection: Induced resistance. J. Cell Mol. Biol. 3:61-69.

El-Gebali, S., Mistry, J., Bateman, A., Eddy, S. R., Luciani, A., Potter, S. C., Qureshi, M., Richardson, L. J., Salazar, G. A., Smart, A., Sonnhammer, E. L. L., Hirsh, L., Paladin, L., Piovesan, D., Tosatto, S. C. E., and Finn, R. D. 2019. The Pfam protein families database in 2019. Nucleic Acids Res. 47:D427-D432.

Ellis, J. G., Rafiqi, M., Gan, P., Chakrabarti, A., and Dodds, P. N. 2009. Recent progress in discovery and functional analysis of effector proteins of fungal and oomycete plant pathogens. Curr. Opin. Plant Biol. 12: 399-405.

Elmore, M. G., Banerjee, S., Pedley, K. F., Ruck, A., and Whitham, S. A. 2020. De novo transcriptome of *Phakopsora pachyrhizi* uncovers putative effector repertoire during infection. Physiol. Mol. Plant Pathol. 110:101464.

Garcia, A., Calvo, É. S., de Souza Kiihl, R. A., Harada, A., Hiromoto, D. M., and Vieira, L. G. E. 2008. Molecular mapping of soybean rust (*Phakopsora pachyrhizi*) resistance genes: Discovery of a novel locus and alleles. Theor. Appl. Genet. 117:545-553.

Germain, H., Joly, D. L., Mireault, C., Plourde, M. B., Letanneur, C., Stewart, D., Morency, M.-J., Petre, B., Duplessis, S., and Séguin, A. 2018. Infection assays in *Arabidopsis* reveal candidate effectors from the poplar rust fungus that promote susceptibility to bacteria and oomycete pathogens. Mol. Plant Pathol. 19:191-200.

Godfrey, D., Böhlenius, H., Pedersen, C., Zhang, Z., Emmersen, J., and Thordal-Christensen, H. 2010. Powdery mildew fungal effector candidates share N-terminal Y/F/WxC-motif. BMC Genomics 11:317.

Godoy, C. V., Seixas, C. D. S., Soares, R. M., Marcelino-Guimarães, F. C., Meyer, M. C., and Costamilan, L. M. 2016. Asian soybean rust in Brazil: Past, present, and future. Pesqui. Agropecu. Bras. 51:407-421.

Hamamouch, N., Li, C., Hewezi, T., Baum, T. J., Mitchum, M. G., Hussey, R. S., Vodkin, L. O., and Davis, E. L. 2012. The interaction of the novel 30C02 cyst nematode effector protein with a plant β-1,3-endoglucanase may suppress host defence to promote parasitism. J. Exp. Bot. 63: 3683-3695.

Hartwig, E. E. 1986. Identification of a fourth major gene conferring resistance to soybean rust1. Crop Sci. 26:1135.

Henrissat, B. 1991. A classification of glycosyl hydrolases based on amino acid sequence similarities. Biochem. J. 280:309-316.

Hidayat, O. O., and Somaatmadja, S. 1977. Screening of soybean breeding lines for resistance to soybean rust (*Phakopsora pachyrhizi* Sydow). Soybean Rust Newsl. 1:9-22.

Hossain, M. Z., Ishiga, Y., Yamanaka, N., Ogiso-Tanaka, E., and Yamaoka, Y. 2018. Soybean leaves transcriptomic data dissects the phenylpropanoid pathway genes as a defence response against *Phakopsora pachyrhizi*. Plant Physiol. Biochem. 132:424-433.

Hu, R., Fan, C., Li, H., Zhang, Q., and Fu, Y.-F. 2009. Evaluation of putative reference genes for gene expression normalization in soybean by quantitative real-time RT-PCR. BMC Mol. Biol. 10:93.

Jin, W., Horner, H. T., Palmer, R. G., and Shoemaker, R. C. 1999. Analysis and mapping of gene families encoding β-1,3-glucanases of soybean. Genetics 153:445-452.

Kitajima S. and Sato F.. 1999. Plant pathogenesis-related proteins: Molecular mechanisms of gene expression and protein function. J. Biochem. 125: 1-8.

Klarzynski, O., Plesse, B., Joubert, J. M., Yvin, J. C., Kopp, M., Kloareg, B., and Fritig, B. 2000. Linear β-1,3 glucans are elicitors of defense responses in tobacco. Plant Physiol. 124:1027-1038.

Kunjeti, S. G., Iyer, G., Johnson, E., Li, E., Broglie, K. E., Rauscher, G., and Rairdan, G. J. 2016. Identification of *Phakopsora pachyrhizi* candidate effectors with virulence activity in a distantly related pathosystem. Front. Plant Sci. 7:269.

Li, S., Smith, J. R., Ray, J. D., and Frederick, R. D. 2012. Identification of a new soybean rust resistance gene in PI 567102B. Theor. Appl. Genet. 125:133-142.

Liao, Y., Zou, H.-F., Wei, W., Hao, Y.-J., Tian, A.-G., Huang, J., Liu, Y.-F., Zhang, J.-S., and Chen, S.-Y. 2008. Soybean *GmbZIP44*, *GmbZIP62* and *GmbZIP78* genes function as negative regulator of ABA signaling and confer salt and freezing tolerance in transgenic *Arabidopsis*. Planta 228:225-240.

Link, T. I., Lang, P., Scheffler, B. E., Duke, M. V., Graham, M. A., Cooper, B., Tucker, M. L., van de Mortel, M., Voegele, R. T., Mendgen, K., Baum, T. J., and Whitham, S. A. 2014. The haustorial transcriptomes of *Uromyces appendiculatus* and *Phakopsora pachyrhizi* and their candidate effector families. Mol. Plant Pathol. 15:379-393.

Linthorst, H. J. M., Melchers, L. S., Mayer, A., van Roekel, J. S., Cornelissen, B. J. C., and Bol, J. F. 1990. Analysis of gene families encoding acidic and basic β-1,3-glucanases of tobacco. Proc. Natl. Acad. Sci. 87:8756-8760.

Luster, D. G., McMahon, M. B., Carter, M. L., Fortis, L. L., and Nuñez, A. 2010. Proteomic analysis of germinating urediniospores of *Phakopsora pachyrhizi*, causal agent of Asian soybean rust. Proteomics 10: 3549-3557.

Ma, S., Niu, H., Liu, C., Zhang, J., Hou, C., and Wang, D. 2013. Expression stabilities of candidate reference genes for RT-qPCR under different stress conditions in soybean. K. Mills, ed. PLoS One 8:e75271.

Mazarei, M., Elling, A. A., Maier, T. R., Puthoff, D. P., and Baum, T. J. 2007. GmEREBP1 Is a transcription factor activating defense genes in soybean and *Arabidopsis*. Mol. Plant-Microbe Interact. 20:107-119.

Mazarei, M., Puthoff, D. P., Hart, J. K., Rodermel, S. R., and Baum, T. J. 2002. Identification and characterization of a soybean ethylene-responsive element-binding protein gene whose mRNA expression changes during soybean cyst nematode infection. Mol. Plant-Microbe Interact. 15: 577-586.

Minh, B. Q., Schmidt, H. A., Chernomor, O., Schrempf, D., Woodhams, M. D., von Haeseler, A., and Lanfear, R. 2020. IQ-TREE 2: New models and efficient methods for phylogenetic inference in the genomic era. Mol. Biol. Evol. 37:1530-1534.

Minic, Z. 2008. Physiological roles of plant glycoside hydrolases. Planta 227:723-740.

Morales, A. M. A. P., O'Rourke, J. A., van de Mortel, M., Scheider, K. T., Bancroft, T. J., Borém, A., Nelson, R. T., Nettleton, D., Baum, T. J., Shoemaker, R. C., Frederick, R. D., Abdelnoor, R. V., Pedley, K. F., Whitham, S. A., and Graham, M. A. 2013. Transcriptome analyses and virus induced gene silencing identify genes in the *Rpp4*-mediated Asian soybean rust resistance pathway. Funct. Plant Biol. 40:1029.

Nielsen, H., Engelbrecht, J., Brunak, S., and von Heijne, G. 1997. Identification of prokaryotic and eukaryotic signal peptides and prediction of their cleavage sites. Protein Eng. Des. Sel. 10:1-6.

Okinaka, Y., Mimori, K., Takeo, K., Kitamura, S., Takeuchi, Y., Yamaoka, N., and Yoshikawa, M. 1995. A structural model for the mechanisms of elicitor release from fungal cell walls by plant β-1,3-endoglucanase. Plant Physiol. 109:839-845.

Opassiri, R., Pomthong, B., Onkoksoong, T., Akiyama, T., Esen, A., and Ketudat Cairns, J. R. 2006. Analysis of rice glycosyl hydrolase family 1 and expression of Os4bglu12 β-glucosidase. BMC Plant Biol. 6:1-19.

Padgitt-Cobb, L. K., Kingan, S. B., and Henning, J. A. 2020. Genomic analysis of powdery mildew resistance in a hop (*Humulus lupulus* L.) biparental population segregating for "R6-locus.". Euphytica 216:10.

Panthee, D. R., Yuan, J. S., Wright, D. L., Marois, J. J., Mailhot, D., and Stewart, C. N. 2007. Gene expression analysis in soybean in response to the causal agent of Asian soybean rust (*Phakopsora pachyrhizi* Sydow) in an early growth stage. Funct. Integr. Genomics 7:291-301.

Petre, B., Saunders, D. G. O., Sklenar, J., Lorrain, C., Win, J., Duplessis, S., and Kamoun, S. 2015. Candidate effector proteins of the rust pathogen *Melampsora larici-populina* target diverse plant cell compartments. Mol. Plant-Microbe Interact. 28:689-700.

Pfaffl, M. W., Horgan, G. W., and Dempfle, L. 2002. Relative expression software tool (REST) for group-wise comparison and statistical analysis of relative expression results in real-time PCR. Nucleic Acids Res. 30:36e-36.

Pierleoni, A., Martelli, P., and Casadio, R. 2008. PredGPI: A GPI-anchor predictor. BMC Bioinform. 9:392.

Qi, M., Grayczyk, J. P., Seitz, J. M., Lee, Y., Link, T. I., Choi, D., Pedley, K. F., Voegele, R. T., Baum, T. J., and Whitham, S. A. 2018. Suppression or activation of immune responses by predicted secreted proteins of the soybean rust pathogen *Phakopsora pachyrhizi*. Mol. Plant-Microbe Interact. 31:163-174.

Qi, M., Link, T. I., Müller, M., Hirschburger, D., Pudake, R. N., Pedley, K. F., Braun, E., Voegele, R. T., Baum, T. J., and Whitham, S. A. 2016. A small cysteine-rich protein from the Asian soybean rust fungus, *Phakopsora pachyrhizi*, suppresses plant immunity. PLOS Pathog. 12:e1005827.

Rincão, M. P., Carvalho, M. C. D. C. G., Nascimento, L. C., Lopes-Caitar, V. S., Carvalho, K. de, Darben, L. M., Yokoyama, A., Carazzolle, M. F., Abdelnoor, R. V., and Marcelino-Guimarães, F. C. 2018. New insights into *Phakopsora pachyrhizi* infection based on transcriptome analysis in planta. Genet. Mol. Biol. 41:671-691.

Sánchez-Rangel, D., Sánchez-Nieto, S., and Plasencia, J. 2012. Fumonisin B1, a toxin produced by *Fusarium verticillioides*, modulates maize β-1,3-glucanase activities involved in defense response. Planta 235: 965-978.

Saunders, D. G. O., Win, J., Cano, L. M., Szabo, L. J., Kamoun, S., and Raffaele, S. 2012. Using hierarchical clustering of secreted protein families to classify and rank candidate effectors of rust fungi. PLoS One 7:e29847.

Schneider, K. T., van de Mortel, M., Bancroft, T. J., Braun, E., Nettleton, D., Nelson, R. T., Frederick, R. D., Baum, T. J., Graham, M. A., and Whitham, S. A. 2011. Biphasic gene expression changes elicited by *Phakopsora pachyrhizi* in soybean correlate with fungal penetration and haustoria formation. Plant Physiol. 157:355-371.

Sekhwal, M. K., Sharma, V., and Sarin, R. 2013. Annotation of glycoside hydrolases in sorghum bicolor using proteins interaction approach. J. Proteome Sci. Comput. Biol. 2:2.

Shi, F., Wang, Y., Zhang, F., Yuan, X., Chen, H., Chen, X., Chen, X., and Cui, X. 2020. Soybean endo-1,3-β-glucanase (GmGLU) interaction with soybean mosaic virus–encoded P3 protein may contribute to the intercelluar movement. Front. Genet. 11:1-12.

Simões, K., Dietrich, S. M. C., Hahn, M. G., and Braga, M. R. 2005. Purification and characterization of a phytoalexin elicitor from spores of the saprobe *Mucor ramosissimus*. Rev. Bras. Botânica. 28:735-744.

Singh, B. B., and Thapliyal, P. N. 1977. Breeding for resistance to soybean rust in India. Pages 62-65 in: Rust of Soybean: The Problem and Research Needs. Report of a workshop held in Manila, The Philippines. R. Ford and J. Sinclair, eds. University of Illinois Urbana-Champagne, Champagne, IL, U.S.A.

Sohn, K. H., Lei, R., Nemri, A., and Jones, J. D. G. 2007. The downy mildew effector proteins ATR1 and ATR13 promote disease susceptibility in *Arabidopsis thaliana*. Plant Cell 19:4077-4090.

Stenflo, J., Stenberg, Y., and Muranyi, A. 2000. Calcium-binding EGF-like modules in coagulation proteinases: Function of the calcium ion in module interactions. BBA-Protein Struct. M. 1477:51-63.

Sticher, L., Hinz, U., Meyer, A. D., and Meins, F. 1992. Intracellular transport and processing of a tobacco vacuolar β-1,3-glucanase. Planta 188: 559-565.

Stone, C. L., McMahon, M. B., Fortis, L. L., Nuñez, A., Smythers, G. W., Luster, D. G., and Frederick, R. D. 2012. Gene expression and proteomic analysis of the formation of *Phakopsora pachyrhizi* appressoria. BMC Genomics 13:269.

van de Mortel, M., Recknor, J. C., Graham, M. A., Nettleton, D., Dittman, J. D., Nelson, R. T., Godoy, C. V., Abdelnoor, R. V., Almeida, Á. M. R., Baum, T. J., and Whitham, S. A. 2007. Distinct biphasic mRNA changes in response to Asian soybean rust infection. Mol. Plant-Microbe Interact. 20:887-899.

Wanderley-Nogueira, A. C., Belarmino, L. C., Soares-Cavalcanti, N. D. M., Bezerra-Neto, J. P., Kido, E. A., Pandolfi, V., Abdelnoor, R. V., Binneck, E., Carazzole, M. F., and Benko-Iseppon, A. M. 2012. An overall evaluation of the resistance (R) and pathogenesis-related (PR) superfamilies in soybean, as compared with Medicago and Arabidopsis. Genet. Mol. Biol. 35:260-271.

Wang, B., Sun, Y., Song, N., Zhao, M., Liu, R., Feng, H., Wang, X., and Kang, Z. 2017. *Puccinia striiformis* f. sp. *tritici* microRNA-like RNA 1 (*Pst*-milR1), an important pathogenicity factor of *Pst*, impairs wheat resistance to *Pst* by suppressing the wheat pathogenesis-related 2 gene. New Phytol. 215:338-350.

Xu, X., Feng, Y., Fang, S., Xu, J., Wang, X., and Guo, W. 2016. Genome-wide characterization of the β-1,3-glucanase gene family in *Gossypium* by comparative analysis. Sci. Rep. 6:29044.

Yamaguchi, T., Nakayama, K., Hayashi, T., Tanaka, Y., and Koike, S. 2002. Molecular cloning and characterization of a novel β-1,3-glucanase gene from rice. Biosci. Biotechnol. Biochem. 66:1403-1406.

Zavaliev, R., Levy, A., Gera, A., and Epel, B. L. 2013. Subcellular dynamics and role of arabidopsis β-1,3-glucanases in cell-to-cell movement of tobamoviruses. Mol. Plant-Microbe Interact. 26:1016-1030.

Zhang, Y., Wei, J., Qi, Y., Li, J., Amin, R., Yang, W., and Liu, D. 2020. Predicating the effector proteins secreted by *Puccinia triticina* through transcriptomic analysis and multiple prediction approaches. Front. Microbiol. 11:1-14.

Zhao, M., Wang, J., Ji, S., Chen, Z., Xu, J., Tang, C., Chen, S., Kang, Z., and Wang, X. 2018. Candidate effector Pst_8713 impairs the plant immunity and contributes to virulence of *Puccinia striiformis* f. sp. *tritici*. Front. Plant Sci. 9:1-15.

Zhong, Y., Wang, B., Yan, J., Cheng, L., Yao, L., Xiao, L., and Wu, T. 2014. DL-β-aminobutyric acid-induced resistance in soybean against *Aphis glycines* Matsumura (Hemiptera: Aphididae). PLoS One 9:e85142.